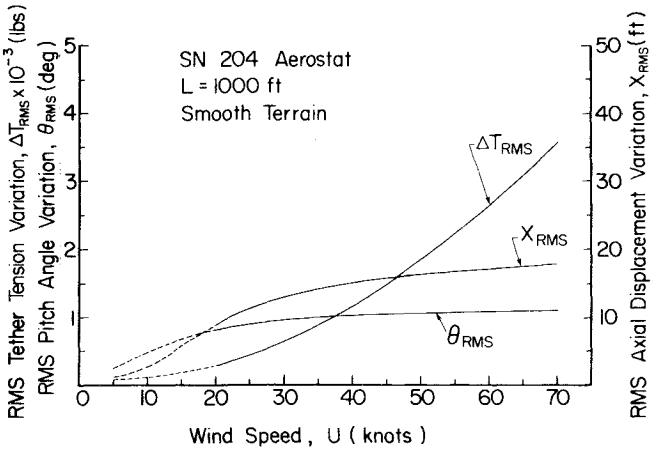

Fig. 2 Predicted rms longitudinal response to atmospheric turbulence.

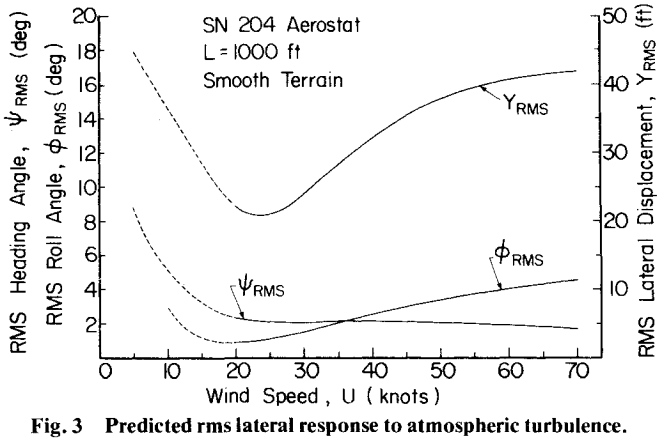

Fig. 3 Predicted rms lateral response to atmospheric turbulence.

and the resulting responses for a wind-speed range of 5 to 70 knots are given in Figs. 2 and 3. Note that the long-wavelength assumption is violated at U_0 below 20 knots. Therefore the dashed portions of the curves are only qualitative variations.

Upon comparison of Figs. 2 and 3, one sees that lateral displacement, y_{rms}, is generally twice the magnitude of the axial displacement, x_{rms}; similarly, the heading angle, ψ_{rms}, is approximately twice as sensitive to turbulence as the pitch angle variation, θ_{rms}. This behavior was qualitatively observed during the SN 204's flight tests. Furthermore, the w_g excitation was over twice as effective as u_g for producing axial responses, and was nearly 10 times as effective in producing pitch responses. Finally, it was found that ΔT_{rms} was due primarily to $\Delta\theta_{rms}$ so that

$$\Delta T_{rms} \cong \frac{\rho U_0^2 S}{2} C_{L_\alpha} \Delta\theta_{rms} \tag{25}$$

Note the alarming increase in ΔT_{rms} with U_0, even for this "smooth-terrain" case. It is clear that configuration redesign to lower θ_{rms} would reduce the required cable safety factor, and hence its weight and drag.

Concluding Remarks

The most important restrictions on the physical model are the long-wavelength assumption and the massless, dragless cable assumption. For aerostats the size of the SN 204, these constrain the validity of this analysis to wind speeds above 20 knots and cable lengths less than 1500 ft. Within this envelope, however, the physical model is well justified, and the analysis should predict an aerostat's behavior with reasonable accuracy.

Currently, this analysis is being used to develop aerostat configurations that will have minimum response to turbulence and hence maximum station-keeping ability. The results from this work will be the subject of a future report.

References

[1]Garlicki, A. and Richenhaller, J., "Logging with Balloons and Helicopters – An Annotated Bibliography," Forest Management Service, Ottawa, Ontario, Canada, Information Report FMR-X-69, Feb. 1975.

[2]Reed, H.E., "A Balloon Transport System," AIAA Paper 75-926, *AIAA Lighter-than-Air Technology Conference,* Snowmass, Colorado, July 15-17, 1975.

[3]Anon., "Tethered Balloon Used for Signal Relay," *Aviation Week and Space Technology,* Vol. 100, April 29, 1974, pp. 52-53.

[4]McLaren, E.J., private communication, Canada Centre for Remote Sensing, Ottawa, Canada, Sept. 1976.

[5]Mickle, R.E. and Davison, D.F., "Results from Sea Trials of a New Boundary-Layer Tethersonde Package," presented at the *Eighth Annual Congress of the Canadian Meteorological Society,* Toronto, Canada, May 30, 1974.

[6]DeLaurier, J.D., "A Stability Analysis for Tethered Aerodynamically Shaped Balloons," *Journal of Aircraft*, Vol. 9, Sept. 1972, pp. 646-651.

[7]DeLaurier, J.D., "Refinements and Experimental Comparisons of a Stability Analysis for Aerodynamically-Shaped Tethered Balloons," AIAA Paper 75-943, *AIAA Lighter-than-Air Technology Conference,* Snowmass, Colorado, July 15-17, 1975.

[8]DeLaurier, J.D., "An Analytical Method for Predicting a Tethered Aerostat's Lateral Response to Atmospheric Turbulence," *Proceedings Ninth AFGL Scientific Balloon Symposium*, Air Force Geophysics Laboratory, Oct. 1976.

[9]Etkin, B., "Flight in Turbulent Air," *Dynamics of Flight*, Wiley, New York, 1966, pp. 310-340.

[10]Ashley, H., "Small Perturbation Response and Dynamic Stability of Flight Vehicles," *Engineering Analysis of Flight Vehicles*, Addison-Wesley, Menlo Park, Calif. 1974, pp. 173-202.

[11]Teunissen, H.W., "Characteristics of the Mean Wind and Turbulence in the Planetary Boundary Layer," UTIAS Review No. 32, Oct., 1970, University of Toronto's Institute for Aerospace Studies, Downsview, Ontario.

Thrust Augmenting Ejector Analogy

Hermann Viets*
Wright State University, Dayton, Ohio

THRUST augmentation sometimes has been viewed by those not directly involved as a violation of basic principles, i.e., something for nothing. This is probably because the total momentum at the ejector exit is greater than the input momentum, a situation which is intuitively disquieting. It is the purpose of this Note to illustrate the same effect in terms of colliding railroad cars and thereby to put thrust augmentation and some of the attendant details on a more intuitive footing. This is a timely objective since a prototype aircraft employing thrust augmentation is currently under construction by Rockwell International for the U.S. Navy.

A schematic of a thrust augmenting ejector is shown in Fig. 1. The primary nozzle is placed within the ejector shroud and expells high-pressure air. The mixing of the surrounding air with the primary air causes a low-pressure region downstream of the nozzle exit which causes ambient air to be entrained into the ejector. The primary and entrained flows are mixed

Received June 25, 1976; revision received Oct. 25, 1976.

Index catagories: Airbreathing Propulsion, Subsonic and Supersonic; Nozzle and Channel Flow; VTOL Powerplant Design and Installation.

*Associate Professor. Associate Fellow AIAA.

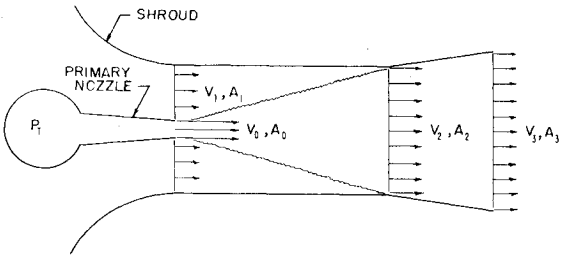

Fig. 1 The ejector principle.

and diffused. The thrust produced by such a device is equal to the momentum at the ejector exit which is greater than the thrust which could be produced by the primary nozzle alone, hence the term thrust *augmentation.*

The production of an output momentum greater than the input momentum may be illustrated simply by considering the inelastic collision of two railroad cars as shown in Fig. 2a. Two cars of mass M_0 and M_1 with velocities V_0 and V_1, respectively, collide inelastically so that the result is a combined mass of (M_0+M_1) moving at a velocity V_2. The governing equations are

$$M_0+M_1=M_2 \tag{1}$$

$$M_0V_0+M_1V_1=M_2V_2 \tag{2}$$

$$M_0V_0^2/2+M_1V_1^2/2=H+M_2V_2^2/2 \tag{3}$$

where H is the amount of energy dissipated to heat during the inelastic collision process. The dissipation H is required since the only way the three equations can be satisfied simultaneously with $H=0$ (i.e. no impact loss) is in the trivial case $V_0=V_1=V_2$. Therefore, even in cases where there are no other losses, the impact loss is inescapable.

Now consider the inelastic collision to take place after both cars have been accelerated down an incline as illustrated in Fig. 2b. The impact takes place at a lower elevation, with both cars at higher velocity, and the two cars together are decelerated as they return to the same initial level. Coming down the incline, assuming no resistance to the motion of the cars, the total energy is conserved

$$V_0^2=V_0'^2+2gh \tag{4a}$$

$$V_1^2=V_1'^2+2gh \tag{4b}$$

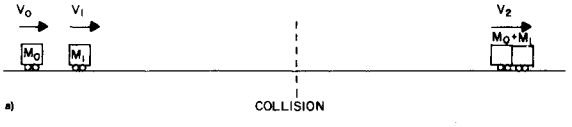

Fig. 2a Analogy of colliding railroad cars.

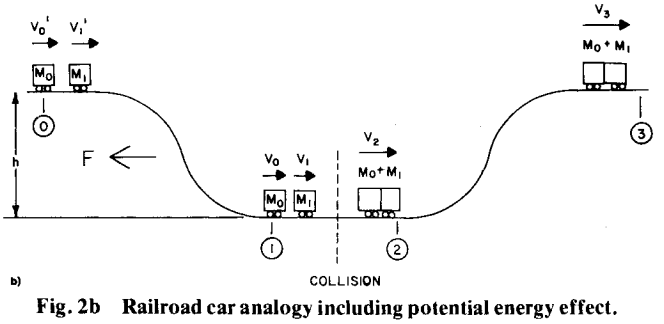

Fig. 2b Railroad car analogy including potential energy effect.

Conserving total energy (i.e. no resistance) coming back up the hill

$$V_3^2=V_2^2-2gh \tag{5}$$

Relating the energy at position 3 to that at position 0, their ratio is the efficiency of the energy transfer occurring between those positions.

$$\eta=\frac{\bar{m}^2+(1-\bar{m})^2\bar{V}^2+2\bar{m}(1-\bar{m})[(1+S^2)^{1/2}(\bar{V}^2+S^2)^{1/2}-S^2]}{\bar{m}^2+(1-\bar{m})^2\bar{V}^2+\bar{m}(1-\bar{m})(1+\bar{V}^2)} \tag{6}$$

where

$$\bar{m}=M_0/(M_0+M_1) \quad S^2=2gh/V_0'^2 \quad \bar{V}=V_1'/V_0'$$

It may be seen from Eq. (6) that the efficiency is maximized at unity when the initial velocity ratio $\bar{V}$ is unity. This suggests that for unequal initial velocities, the transfer efficiency may be improved by lowering the depression h, as is verified by the computations in Fig. 3a, for $m=0.1$ and various velocity ratios.

The ratio of the momentum at position 3 in Fig. 2b to that at position 0 is

$$\phi=M_3V_3/M_0V_0=V_3/\bar{m}V_0 \tag{7}$$

but

$$\eta=V_3^2/\bar{m}V_0^2 \tag{8}$$

so

$$\phi=(1/\bar{m})[\bar{m}\eta]^{1/2} \tag{9}$$

Now for the simplest case of a moving body striking a stationary body ($\bar{V}=0$) on level ground ($S=0$), Eqs. (6) and (9) reduce to

$$\eta=\bar{m} \qquad \phi=\sqrt{\eta/\bar{m}} \tag{10}$$

so the momentum is, of course, conserved. However, if the same collision occurs after the cars have been accelerated down the incline S (one car starting from rest), then

$$\eta=\frac{\bar{m}^2+2\bar{m}(1-\bar{m})[(1+S^2)^{1/2}S-S^2]}{\bar{m}^2+\bar{m}(1-\bar{m})} \tag{11}$$

The resulting variation in ϕ with the speed ratio S is shown in Fig. 3b. Thus, it may be seen that the resultant momentum at position 3 is greater than that at 1 and a thrust augmentation has been effected.

The analogy to thrust augmenting ejectors is this: the primary mass flow M_0 collides with the secondary mass flow M_1. The efficiency with which this process can be undertaken can be improved if the flows are accelerated so that the velocity difference between them, at collision, is minimized. This is precisely the role of the ejector shroud – to lower the static pressure within the mixing region and thereby accelerate the ambient air into the device. Thus, the elevation is analogous to the pressure within the ejector, the decrease occurring in the inlet and the increase in the diffuser.

Of course in the real case, there are losses due to friction both for the case of the cars and the ejector. In the case of the colliding masses, the track friction and drag losses make it more difficult for the combined cars, after the collision, to climb back up the hill. If the cars have insufficient energy to reach the top of the diffuser incline, they fall back. This is analogous to diffuser stall, where the flow near the wall has

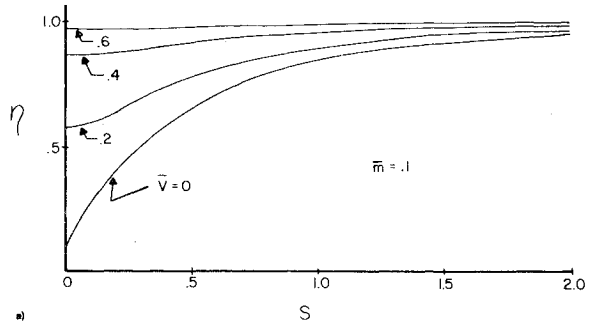

Fig. 3a Variation of transfer efficiency with speed ratio.

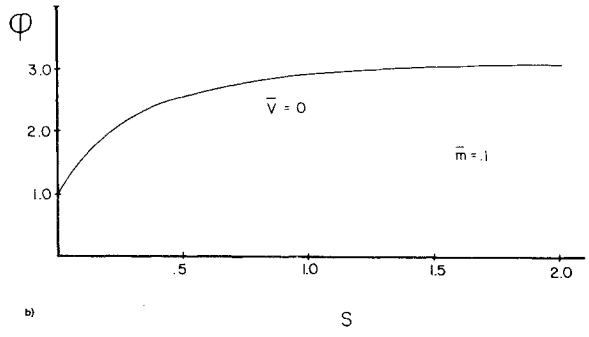

Fig. 3b Variation of thrust (momentum) augmentation with speed ratio.

insufficient energy to overcome the pressure gradient in the diffuser.

Since the momentum at position 3 is greater than that at 0, there must be a net force to the left on the earth supporting the track arrangement. This is analogous to the force transmitted to the ejector shroud by the internal pressure distribution which becomes the usable force on the aircraft.

The relative effect of inlet area ratio may be seen in the mass ratio $\bar{m}$. A small $\bar{m}$ corresponds to a high inlet area ratio and leads (in the ideal, no-loss case) to improved performance. The analogy to the primary nozzle thrust efficiency is the ratio of the actual velocity of mass M_0 at position 1 to its velocity at that position with no friction losses. The difference between these velocities is analogous to the flow losses within the primary nozzle system.

Thus, in this analogy, the basic mechanism responsible for thrust augmentation clearly may be identified as the improved transfer efficiency from the primary to the secondary because of the presence of the shroud which accelerates the secondary and decreases the velocity difference. However, the optimization of this process in the presence of various loss mechanisms is not straightforward because of the many parametric interactions involved.

Experiments Concerning Free-Fall Simulation

M. J. Houghton*
The University of Southampton, Southampton, England

A Vertical Wind Tunnel

THE aerodynamics and limitations of the human body in free fall is an interesting[1] and potentially important[2] area for research. A proposal has been made[2] concerning a vertical wind tunnel, specially designed to establish those conditions pertaining to free-fall parachuting, in which a student parachutist can develop his skills without danger of serious collision with the surrounding wind tunnel structure. The major advantages over conventional free-fall training are: a) safety, b) cheapness, c) time saving (e.g. weather independent operation), d) nonspecialist training and in evaluating free-fall stabilizing equipment (drogues, etc.) for inexperienced or heavily laden free fallers.

Here it is emphasized that this facility provides a very useful research tool allowing easy access to the air flow in a "nonhostile" laboratory environment; operation of the simulator for 1 hour is equivalent to 120 conventional descents from 7,000 ft. in terms of free-fall time.

The essential features of the simulator are: 1) a negative vertical velocity gradient – induced by the funnel shaped working section (axis a b is vertical); 2) a positive radial velocity gradient-induced by suitable ducts or windmills (not shown in Fig. 1a) inside the effuser. Features (1) and (2) imply that the equilibrium of the free faller ("Suspended" by the vertical airflow) is stable against induced vertical and horizontal displacements; a harness is essential for exercises, or studies, involving horizontal "tracking" – a strain gage measuring performance.

Stable equilibrium was indicated experimentally by the motion-free suspension of a free-falling shuttlecock (or table tennis ball etc.) within the center of the working section of Fig. 1b. Unfortunately the power requirement for a full scale

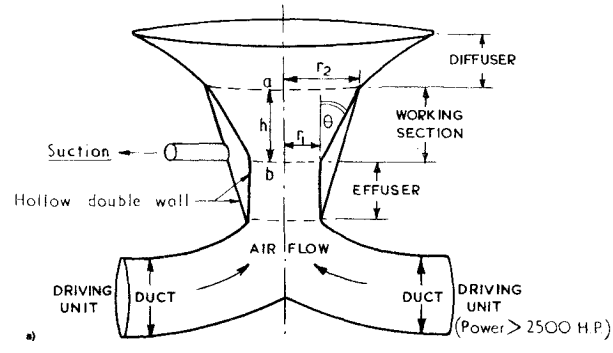

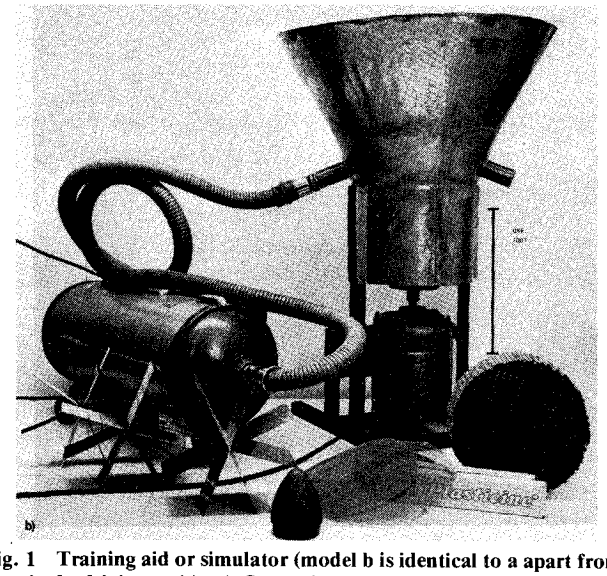

Fig. 1 Training aid or simulator (model b is identical to a apart from the single driving unit). a) Open circuit version, side view (internal vanes are not indicated). Suction through holes (not shown) in the inner working section wall prevents flow separation[3] which occurs if $\theta > 6°$. b) Working scale model. Vanes, honeycomb, etc. used in eliminating swirl and in shaping the flow velocity profile are shown in the foreground. Plasticine was used to shape the inner working section wall.

Received Oct. 5, 1976; revision received Dec. 7, 1976.
Index categories: Research Facilities and Instrumentation.
*Research Fellow, Space Physics Group, Dept. of Physics.